

# Pre-event Trends in the Panel Event-study Design

Simon Freyaldenhoven, *Federal Reserve Bank of Philadelphia*

Christian Hansen, *University of Chicago*

Jesse M. Shapiro, *Brown University and NBER\**

May 2019

## Online Appendix

### List of Tables

1	Static estimates in non-stationary DGP. . . . .	2
2	Estimates of the effect of newspapers on voter turnout, including covariates. . . . .	3

### List of Figures

1	Simulation results when $z_{it}$ is determined by $\eta_{it}$ and additional noise. . . . .	4
2	Average number of events in simulations. . . . .	5
3	Distribution of event plots for stationary $\eta_{it}$ . . . . .	6
4	Simulation results using BIC to select leads. . . . .	7
5	Simulation results adding unit-specific linear time trends. . . . .	8
6	Rejection probability of pre-test in simulations. . . . .	9
7	Effect of normalization on event plots. . . . .	10
8	Different linear extrapolation methods. . . . .	11
9	Event plots under different pre-testing procedures. . . . .	12
10	Simulation results using $\hat{\delta}_0$ as an estimate for $\beta$ . . . . .	13
11	Estimated effects on voter turnout in presidential election years around newspaper entries/exits, including demographic controls. . . . .	14

---

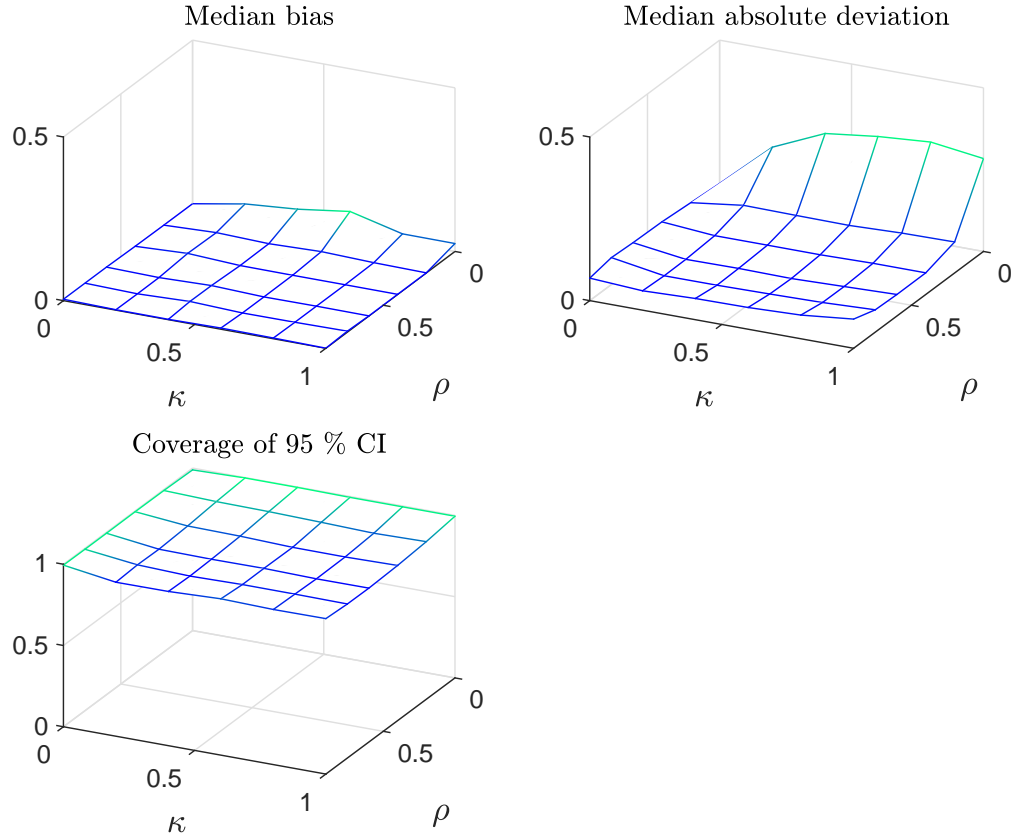
\*Emails: [simon.freyaldenhoven@phil.frb.org](mailto:simon.freyaldenhoven@phil.frb.org), [chansen1@chicagobooth.edu](mailto:chansen1@chicagobooth.edu), [jesse\\_shapiro.1@brown.edu](mailto:jesse_shapiro.1@brown.edu).

Estimator	Median Bias	Median Absolute Deviation	Coverage (95% CIs)
Controlling directly for $\eta_{it}$ (infeasible)	-0.00	0.04	0.96
Failing to control for $\eta_{it}$	0.65	0.65	0.00
Using $x_{it}$ as proxy for $\eta_{it}$	0.47	0.47	0.00
Proposed 2SLS estimator (closest lead)	-0.00	0.11	0.95
Extrapolating a linear trend	-0.07	0.15	0.95
Pre-testing for pre-trend	0.66	0.66	0.41

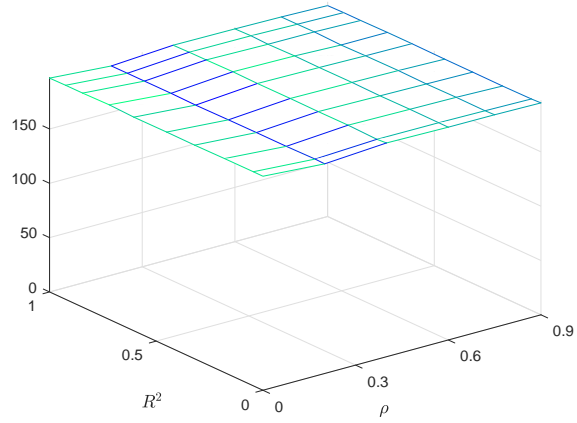
Online Appendix Table 1: Estimates from a static analogue of the dynamic specifications depicted in Figure 3. Specifically, we consider  $y_{it} = \beta z_{it} + \omega_t + \alpha_i + \eta_{it}\gamma + \varepsilon_{it}$ , where  $\omega_t$  are time effects, and the object of interest is the causal effect  $\beta$ . For the linear extrapolation estimator, we use  $\hat{\beta} = \frac{1}{5} \sum_{k=-4}^0 \hat{\delta}_{-k}$ , with  $\delta_k$  from equation (14), as the estimate. Standard errors are clustered at the individual level. Results are based on 5,000 draws from the benchmark DGP defined in Section II.A.

Estimator	Effect of newspaper entry	Coefficient on lead in first stage
No control	0.0034 (0.0009)	
Controlling for $x_{it}$	0.0041 (0.0010)	
Proposed 2SLS estimator (one lead)	0.0029 (0.0014)	0.0079 (0.0013)

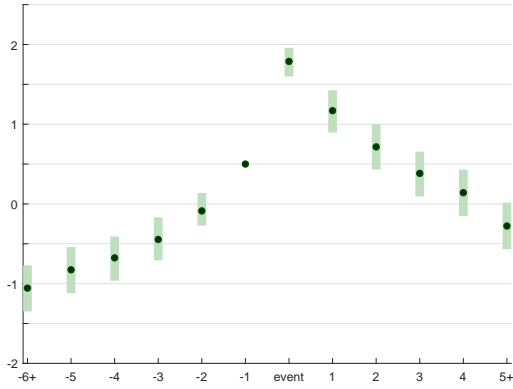
Online Appendix Table 2: Estimates of the effect of newspapers on voter turnout, including covariates. Table depicts estimates  $\hat{\beta}$  of the effect of the number of newspapers on voter turnout from  $\Delta y_{it} = \beta \Delta z_{it} + \Delta \omega_{st} + \gamma \Delta \eta_{it} + \Delta q'_{it} \theta + \Delta \varepsilon_{it}$ . The model differs from the model in the main paper through the inclusion of the vector of covariates  $q_{it}$ . In line with the alternative specification in Gentzkow, Shapiro and Sinkinson (2011), this vector includes the share of the population that is white, the share of the white population that is foreign-born, the share of the population living in cities with 25,000+ residents, the share of the population living in towns with 2,500+ residents, the population employed in manufacturing as a share of males over 21 years old, and the log of manufacturing output per capita (as proxy for income). See Table 2 for definitions of the estimators. Standard errors in parentheses are clustered at the county level.



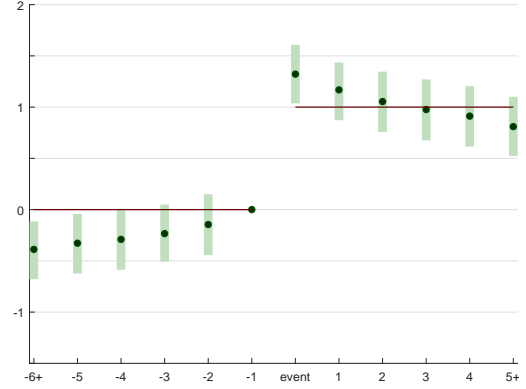
Online Appendix Figure 1: Performance of our proposed estimator (“2SLS - one lead”) when  $z_{it}$  is determined by  $\eta_{it}$  and additional noise. We deviate from the DGPs in Definition 1 and Figures 4 - 6 in assuming that  $z_{it} = \mathbf{1}(\{\exists t^* \leq t : \eta_{it^*}^\dagger > \eta^*\})$ , where  $\eta_{it}^\dagger = \sqrt{\kappa}\eta_{it} + \sqrt{1 - \kappa}\tau_{it}$  and  $\tau_{it} \sim N(0, 1)$  independently of the other variables. To vary the importance of  $\eta_{it}$  in determining  $z_{it}$ , we vary  $\kappa$  from zero to one. We fix the population  $R^2$  from the infeasible regression of  $x_{it}$  on  $\eta_{it}$  in (11) at 0.45. Each figure is based on 2,000 simulation replications. The horizontal axes in each panel correspond to the different values of  $\rho$  and  $\kappa$ .



Online Appendix Figure 2: Average number of cross-sectional observations in which an event occurs across the design space considered in the simulations for Figures 4 - 6. Within each set of simulation parameters, at least 99.4 percent of draws have between 160 and 240 units with an event.

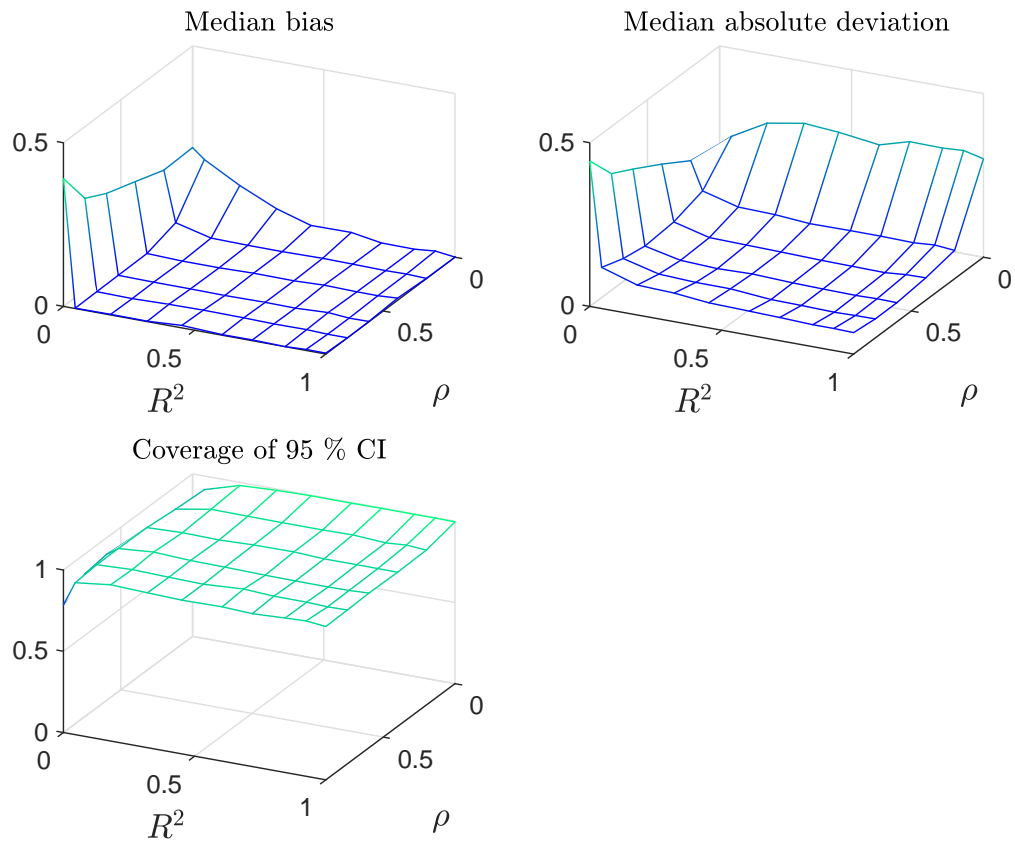


(a) Confound  $\eta_{it}$  around event time

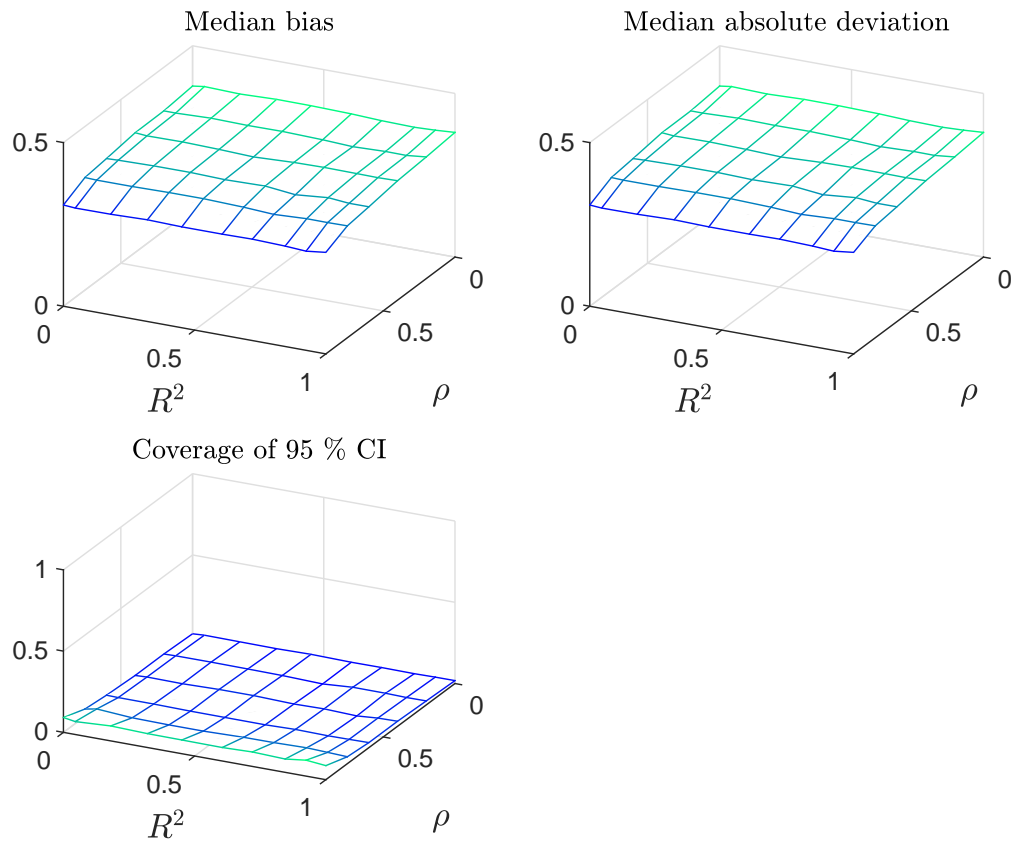


(b) Outcome of interest  $y_{it}$  around event time

Online Appendix Figure 3: Distribution of event plots with stationary  $\eta_{it}$ . Each plot shows estimates of the coefficients  $\delta_k$  from (13) under simulated data from our stationary DGP with  $\rho = 0.75$ . The dots in the center represent the median estimate across 5,000 realizations, while the shaded areas depict the uniform 95% confidence band: 95% of the estimated sets of coefficients lie within this band. The solid line depicts the true causal effect.

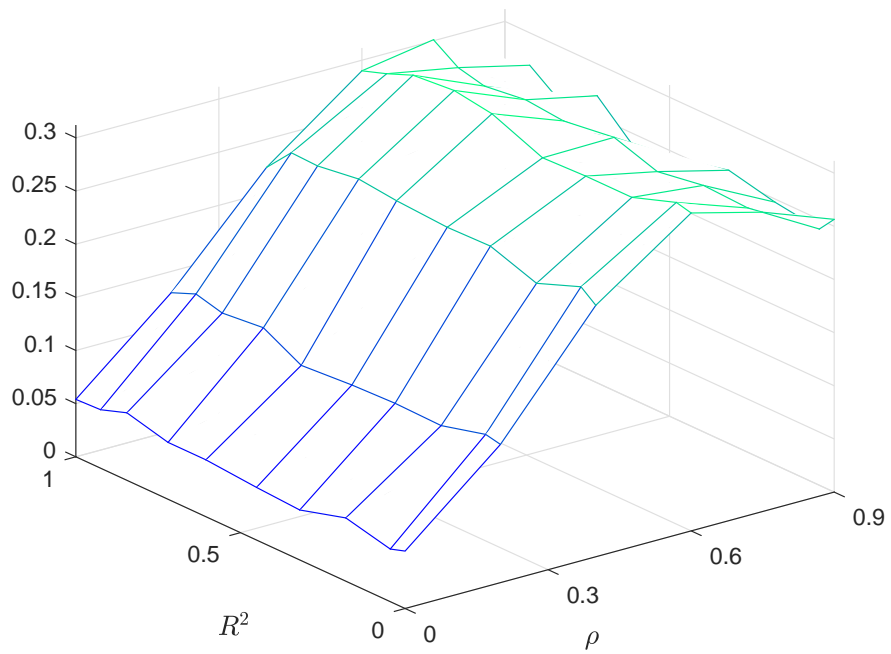


Online Appendix Figure 4: Additional panel for Figures 4 - 6 using the BIC in the first stage to choose the number of leads, between 1 and 5, to be used as excluded instruments.

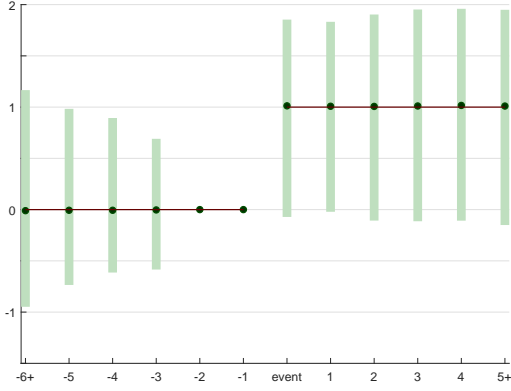


Online Appendix Figure 5: Additional panel for Figures 4 - 6 adding unit-specific linear time trends to the estimating equation. Specifically, we consider an estimate  $\hat{\beta}$  from  $y_{it} = \beta z_{it} + \omega_t + \alpha_i + \xi_i t + \varepsilon_{it}$ , where  $\xi_i$  is the slope of the time trend for unit  $i$ .

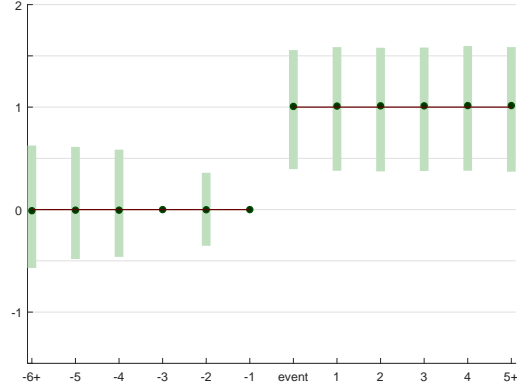




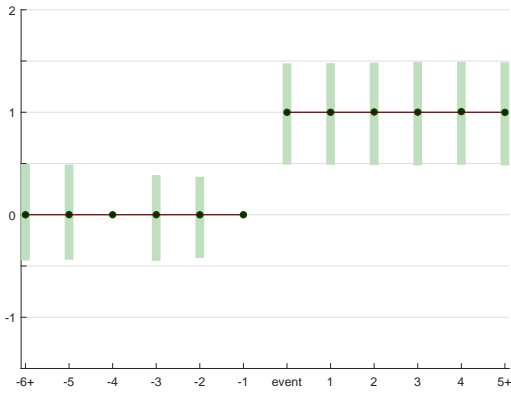
Online Appendix Figure 6: Probability of rejecting the null hypothesis of no pre-trend for panel (f) of Figures 4 - 6. With the event plot normalized such that the coefficient on  $z_{i,t+1}$  is equal to zero, our pre-test tests that the coefficient on  $z_{i,t+2}$  is equal to zero at the 5% level.



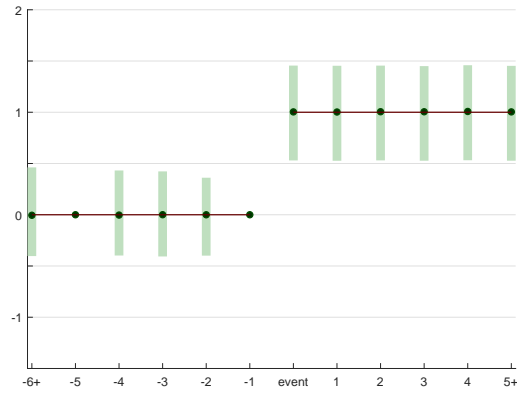
(a) Proposed 2SLS estimator, with closest lead of  $z_{it}$  as excluded instrument. Normalized such that  $\delta_{-1} = \delta_{-2} = 0$ .



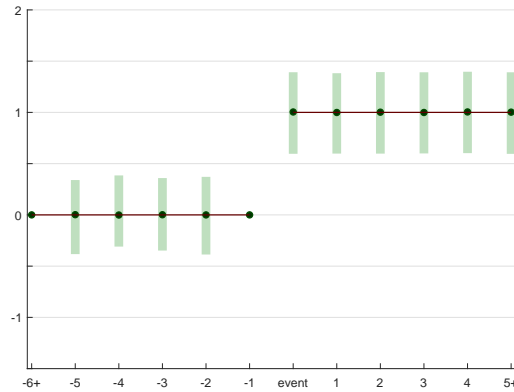
(b) Proposed 2SLS estimator, with closest lead of  $z_{it}$  as excluded instrument. Normalized such that  $\delta_{-1} = \delta_{-3} = 0$ .



(c) Proposed 2SLS estimator, with closest lead of  $z_{it}$  as excluded instrument. Normalized such that  $\delta_{-1} = \delta_{-4} = 0$ .

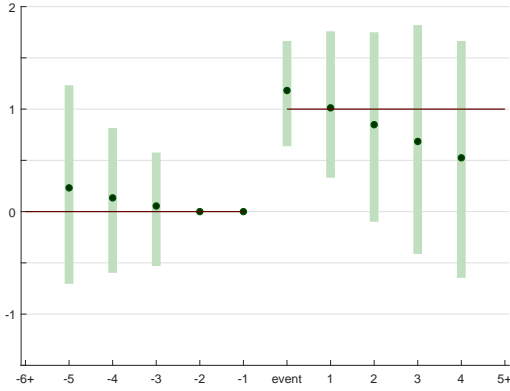


(d) Proposed 2SLS estimator, with closest lead of  $z_{it}$  as excluded instrument. Normalized such that  $\delta_{-1} = \delta_{-5} = 0$ .

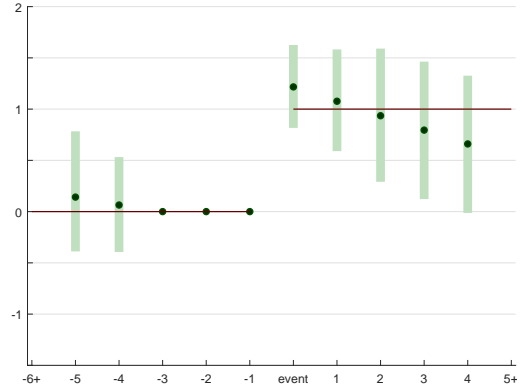


(e) Proposed 2SLS estimator, with closest lead of  $z_{it}$  as excluded instrument. Normalized such that  $\delta_{-1} = \delta_{-6+} = 0$ .

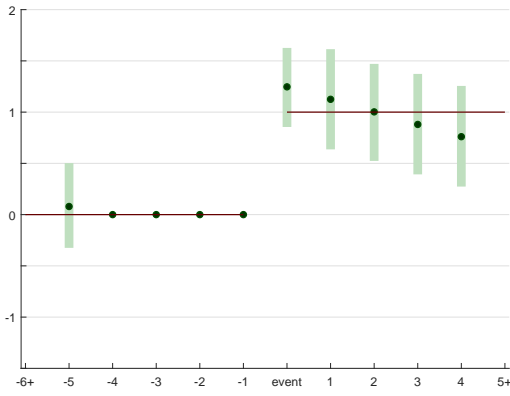
Online Appendix Figure 7: Distribution of event plots under the presence of a confounding factor using different normalizations. Each plot shows estimates of the coefficients  $\delta_k$  from (13) under simulated data from the benchmark DGP defined in Section II.A. The dots in the center represent the median estimate across 5,000 realizations, while the shaded areas depict the uniform 95% confidence band: 95% of the estimated sets of coefficients lie within this band. The solid line depicts the true causal effect. Figure 7a above is identical to Figure 3d in the paper.



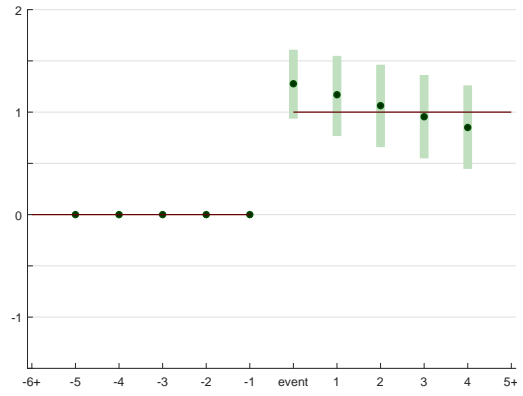
(a) Extrapolating a linear trend from the two periods immediately preceding the event



(b) Extrapolating a linear trend from the three periods immediately preceding the event

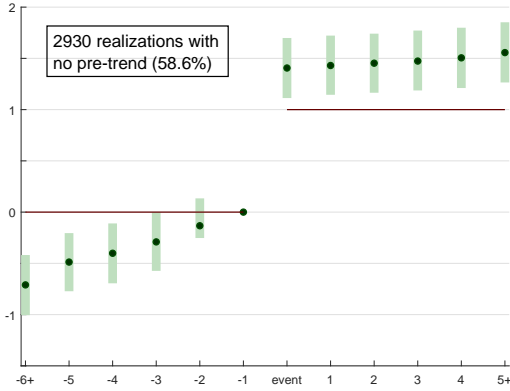


(c) Extrapolating a linear trend from the four periods immediately preceding the event

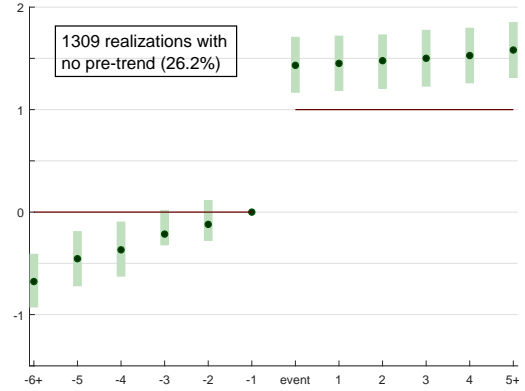


(d) Extrapolating a linear trend from the five periods immediately preceding the event

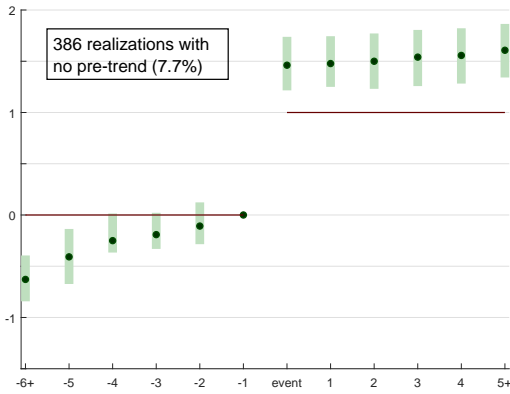
Online Appendix Figure 8: Each plot shows estimates of the coefficients  $\delta_k$  from (14) using a different number of pre-event periods to estimate the linear time trend in event time under simulated data from the benchmark DGP defined in Section II.A. The true causal effect  $\beta$  is equal to one, represented by the solid line. The dots in the center represent the median estimate across 5,000 realizations, while the shaded areas depict the uniform 95% confidence band: 95% of the estimated sets of coefficients lie within this band. Figure 8b above is identical to Figure 3e in the paper.



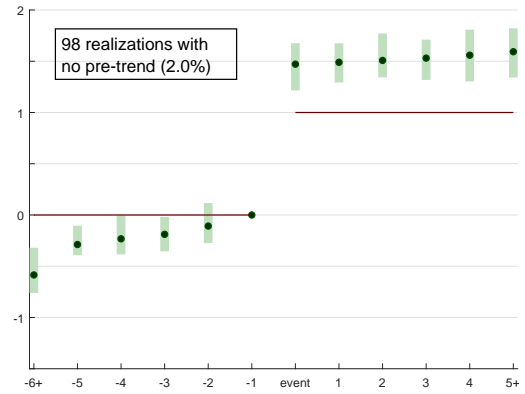
(a) Pre-testing if  $\delta_{-2} = 0$  in (13)



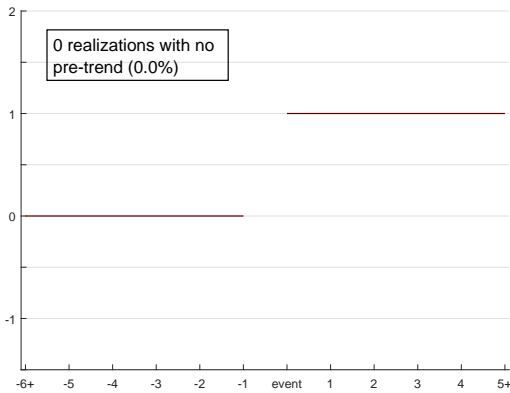
(b) Pre-testing if  $\delta_{-2} = \delta_{-3} = 0$  in (13)



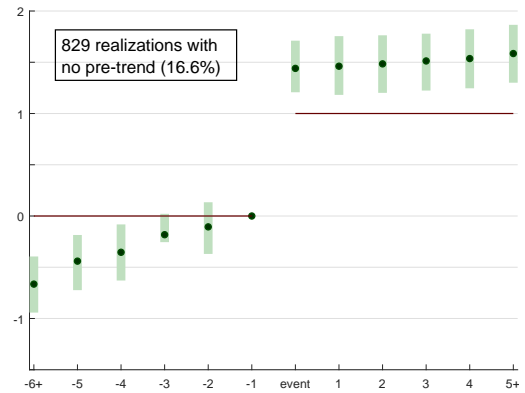
(c) Pre-testing if  $\delta_{-2} = \delta_{-3} = \delta_{-4} = 0$  in (13)



(d) Pre-testing if  $\delta_{-2} = \delta_{-3} = \delta_{-4} = \delta_{-5} = 0$  in (13)

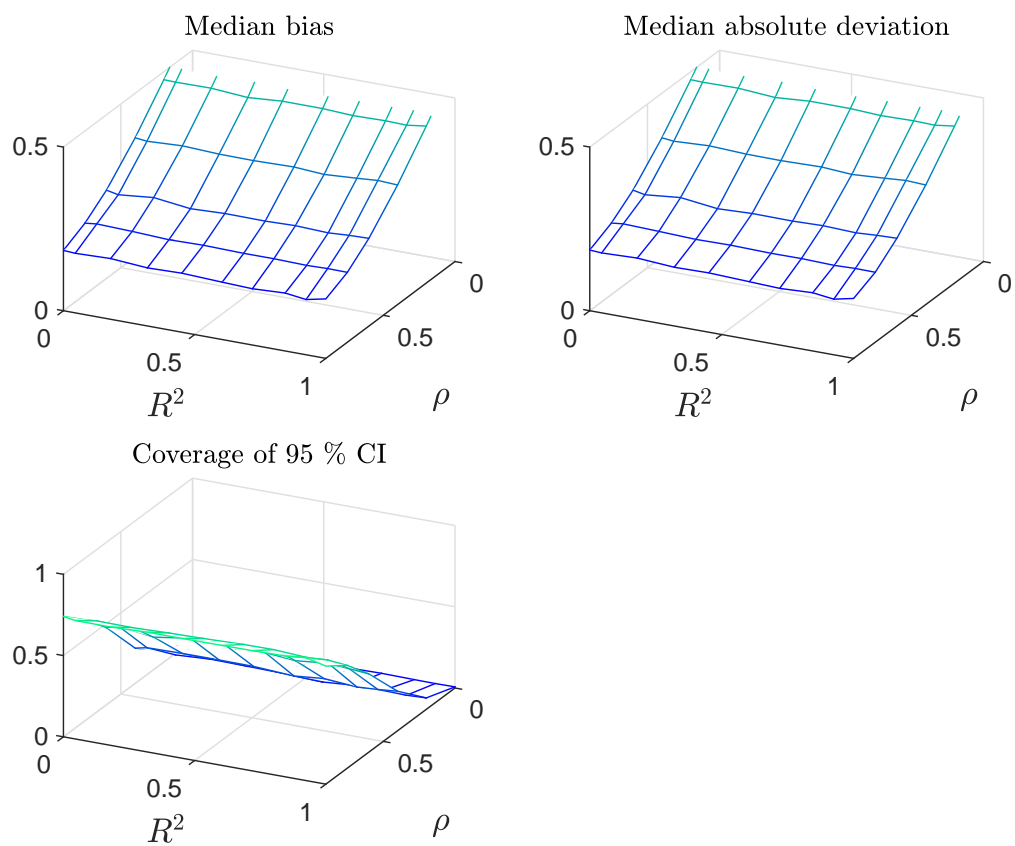


(e) Pre-testing if  $\delta_{-2} = \delta_{-3} = \delta_{-4} = \delta_{-5} = \delta_{-6+} = 0$  in (13)

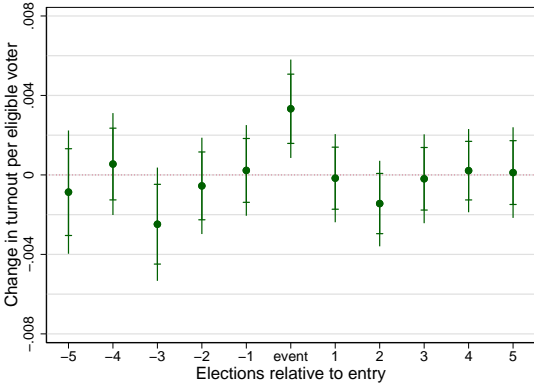


(f) Pre-testing if  $\Omega = 0$  in (14)

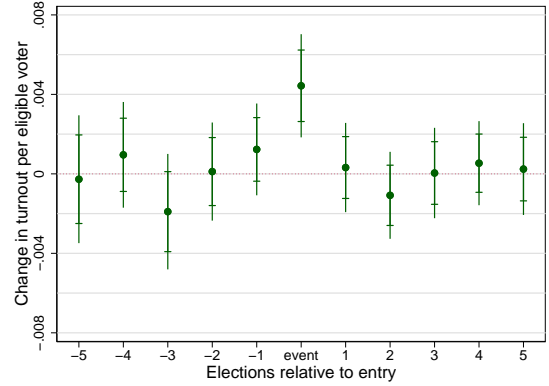
Online Appendix Figure 9: Distribution of event plots after different pre-testing procedures using simulated data. All plots are based on 5,000 simulations of the benchmark DGP defined in Section II.A with a true causal effect of  $\beta = 1$ , represented by the solid line. Each plot shows estimates of the coefficients  $\delta_k$  from (13) ignoring  $\eta_{it}$  after pre-testing for a pre-trend in  $y_{it}$ . All plots are based on those realizations in which we do not detect a pre-trend. The dots in the center represent the median estimate across those realizations, while the shaded areas depict the uniform 95% confidence band: 95% of the estimated sets of coefficients lie within this band. Figure 9a above is identical to Figure 3f in the paper.



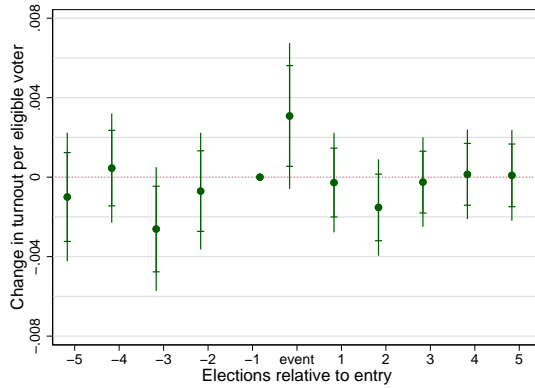
Online Appendix Figure 10: Additional panel for Figures 4 - 6 using  $\hat{\beta} = \hat{\delta}_0$  from the dynamic model in equation (14) as an estimate for the causal effect  $\beta$ .



(a) Not controlling for market profitability



(b) Using the log of voting-eligible population as a proxy for market profitability



(c) Proposed 2SLS estimator, with closest lead of  $z_{it}$  as excluded instrument

Online Appendix Figure 11: Estimated effects on voter turnout in presidential election years around newspaper entries/exits including demographic controls. Figure depicts estimates of the coefficients  $\delta_k$  from three specifications of the equation  $\Delta y_{it} = \sum_{k=-5}^5 \delta_k \Delta z_{i,t-k} + \Delta \omega_{st} + \gamma \Delta \eta_{it} + \Delta q'_{it} \theta + \Delta \varepsilon_{it}$ . The model differs from (19) through the inclusion of the vector of covariates  $q_{it}$ . In line with the alternative specification in Gentzkow, Shapiro and Sinkinson (2011), this vector includes the share of the population that is white, the share of the white population that is foreign-born, the share of the population living in cities with 25,000+ residents, the share of the population living in towns with 2,500+ residents, the population employed in manufacturing as a share of males over 21 years old, and the log of manufacturing output per capita (as proxy for income). Inner confidence sets as indicated by the dashes correspond to 95% pointwise confidence intervals, while outer confidence sets are the uniform 95% sup-t bands (with critical values obtained via simulation). Confidence sets are based on standard errors clustered at the county level.